Importance of the Interlayer Te···Te Contacts on the Electronic Structure of the Layered Telluride $Nb_3Ge_{0.9}Te_6$

E. Canadell*

Laboratoire de Chimie Théorique, Université de Paris-Sud, 91405 Orsay, France

L. Monconduit, M. Evain, R. Brec, and J. Rouxel

Laboratoire de Chimie des Solides, Institut des Matériaux de Nantes, Université de Nantes, 44072 Nantes, France

M.-H. Whangbo*

Department of Chemistry, North Carolina State University, Raleigh, North Carolina 27695-8204

Received May 19, 1992

The electronic structure of the layered telluride $Nb_3Ge_{0.9}Te_6$ was examined by performing tight-binding band calculations on the stoichiometric composition Nb_3GeTe_6. Due to the short interlayer Te···Te contacts, the top part of the Te p_z-block bands of Nb_3GeTe_6 is raised above the Fermi level. This gives rise to a partial p → d electron transfer and to positive overlap populations for the interlayer Te···Te contacts, as in the case of the CdI_2-type ditellurides MTe_2 (M = Ti, Nb). The Fermi surfaces calculated for Nb_3GeTe_6 suggest that $Nb_3Ge_{0.9}Te_6$ is a three-dimensional metal, with its electrical conductivity increasing along the $b < c < a$ axis directions.

In the past few years, synthesis and characterization of transition-metal tellurides have received considerable attention.[1-7] In many layered transition-metal tellurides, interlayer Te···Te contacts are substantially shorter than the van der Waals (VDW) distance of 4.0 Å.[8] The electronic structure studies of the CdI_2-type layered transition-metal ditellurides MTe_2 (M = Ti, Nb, Ir) show[2b,d] that the oxidation state of Te cannot be considered as −2 because of a significant electron transfer from the Te p-block bands to the metal d-block bands (hereafter referred to as the p → d electron transfer). A crucial factor responsible for the p → d electron transfer is the short interlayer Te···Te contacts.[2d] The overlap between the Te p_z orbitals (perpendicular to the layer) for such contacts is generally large due to the diffuse nature of the Te atomic orbitals. The antibonding interactions associated with the short interlayer Te···Te contacts raise the top portion of the Te p-block bands above the Fermi level.[2d] Thus, the Te p-block bands involved in the p → d electron transfer of the CdI_2-type ditellurides MTe_2 are largely made up of the Te p_z orbitals. Consequently, the CdI_2-type ditellurides MTe_2 possess a metallic character along the interlayer direction, and a slight change in the interlayer Te···Te contact arrangements significantly affect the electrical and other physical properties of these ditellurides. These conclusions, observed for the ditellurides MTe_2 in which the metal atoms are in an octahedral environment, may apply equally well to other types of layered transition-metal tellurides.

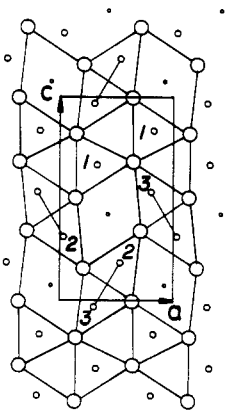

Figure 1. Projection view along the *b*-axis direction of $Nb_3Ge_{0.9}Te_6$, where the large, medium, and small circles represent Te, Nb, and Ge atoms, respectively.

In the layered telluride $Nb_3Ge_{0.9}Te_6$, recently characterized by Monconduit et al.[9] the metal atoms are in a trigonal prismatic coordination. This compound consists of layers made up of $NbTe_6$ trigonal prisms (Figure 1). $Nb_3Ge_{0.9}Te_6$ contains two such prismatic layers per unit cell. There are three kinds of Nb atoms in each prismatic layer of $Nb_3Ge_{0.9}Te_6$, the Nb_2Te_8 double prisms are fused to form chains running along the *a*-axis direction, and these chains are interconnected by the $NbTe_6$ single prisms. The $NbTe_6$ single prisms and the Nb_2Te_8 double prisms are capped by Ge atoms with short Ge···Nb contact distances. This telluride possesses numerous intra- and interlayer Te···Te contacts shorter

(1) For a recent review, see: Böttcher, B. *Angew. Chem. Int. Ed. Engl.* **1988**, *27*, 759.
(2) (a) Jobic, S.; Brec, R.; Rouxel, J. *J. Solid State Chem.* **1992**, *96*, 169. (b) Jobic, S.; Deniard, P.; Brec, R.; Rouxel, J.; Jouanneaux, A.; Fitch, A. N. *Z. Anorg. Allg. Chem.* **1991**, *598/599*, 199. (c) Jobic, S.; Brec, R.; Rouxel, J. *J. Alloys Comp.* **1992**, *178*, 253. (d) Canadell, E.; Jobic, S.; Brec, R.; Rouxel, J. *J. Solid State Chem.* **1992**, *99*, 189. (e) Jobic, S.; Evain, M.; Brec, R.; Deniard, P.; Jouanneaux, A.; Rouxel, J. *J. Solid State Chem.* **1991**, *95*, 319. (f) Whangbo, M.-H.; Canadell, E. *J. Am. Chem. Soc.*, in press.
(3) (a) Liimatta, E. W.; Ibers, J. *J. Solid State Chem.* **1988**, *77*, 141; **1989**, *78*, 7. (b) Mar, A.; Ibers, J. *J. Chem. Soc. Dalton Trans.* **1991**, 639; *J. Solid State Chem.* **1992**, *97*, 166; **1991**, *92*, 352. (c) Keane, P. M.; Ibers, J. *Inorg. Chem.* **1991**, *30*, 3096; *J. Solid State Chem.* **1991**, *93*, 291.
(4) (a) Badding, M. E.; DiSalvo, F. J. *Inorg. Chem.* **1990**, *29*, 3952. (b) Li, J.; Badding, M. E.; DiSalvo, F. J. *Inorg. Chem.* **1992**, *31*, 1050.
(5) Tremel, W. *Angew. Chem., Int. Ed. Engl.* **1991**, *30*, 840; *J. Chem. Soc., Chem. Commun.* **1991**, 1405.
(6) (a) Park, Y.; Degroot, D. C.; Schindler, J.; Kannewurf, C. R.; Kanatzidis, M. G. *Angew. Chem., Int. Ed. Engl.* **1991**, *30*, 1325. (b) Park, Y.; Kanatzidis, M. G. *Chem. Mater.* **1991**, *3*, 781.
(7) Lee, S.; Nagasundaram, N. *Chem. Mater.* **1989**, *1*, 597.
(8) Bondi, A. *J. Phys. Chem.* **1964**, *68*, 441.
(9) Monconduit, L.; Evain, M.; Boucher, F.; Brec, R.; Rouxel, J. *Z. Anorg. Allg. Chem.* **1992**, *616*, 177.

0020-1669/93/1332-0010$04.00/0

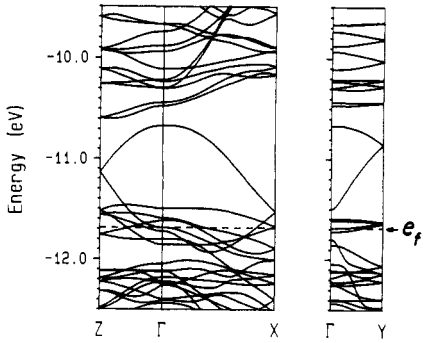

Figure 2. Dispersion relations calculated for Nb_3GeTe_6, where the dashed line refers to the Fermi level appropriate for $Nb_3Ge_{0.9}Te_6$. $\Gamma = (0, 0, 0)$, $X = (a^*/2, 0, 0)$, $Y = (0, b^*/2, 0)$, and $Z = (0, 0, c^*/2)$.

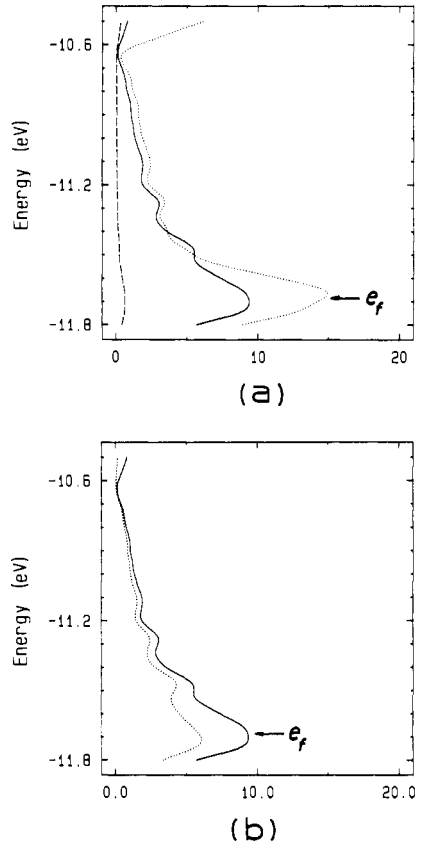

Figure 3. (a) PDOS values of Nb (dotted line), Ge (dashed line) and Te (solid line) calculated for Nb_3GeTe_6. (b) Te p_z-orbital contribution (dotted line) to the PDOS of Te (solid line) calculated for Nb_3GeTe_6.

than the VDW distance of 4.0 Å (for example, 3.766, 3.803, 3.830, and 3.939 Å for interlayer; 3.744, 3.764, 3.782, 3.836, 3.846, and 3.932 Å for intralayer). To see if the interlayer Te···Te contacts of $Nb_3Ge_{0.9}Te_6$ play a role similar to what those of the CdI_2-type ditellurides do, we examined the electronic structure of $Nb_3Ge_{0.9}Te_6$ by performing extended Hückel tight-binding (EHTB) band electronic structure calculations[10] for the stoichiometric composition Nb_3GeTe_6. Not being self-consistent, EHTB calculations are not expected to give a quantitative estimate for the p → d electron transfer. Nevertheless, the atomic parameters employed in the study[2d] of the CdI_2-type ditelluride MTe_2 provide results in agreement with first principles calculations and experimental results. In the present EHTB calculations, these atomic parameters were used for Nb and Te.[11]

The dispersion relations of the electronic energy bands calculated for Nb_3GeTe_6 are shown in Figure 2, where the dashed line represents the Fermi level appropriate for $Nb_3Ge_{0.9}Te_6$ in a rigid band approximation, i.e., for $Nb_3GeTe_6^{0.4+}$. Partially filled bands are present in all three directions Γ-X, Γ-Y and Γ-Z, so that $Nb_3Ge_{0.9}Te_6$ is predicted to be a three-dimensional metal. Analysis of the density of states (DOS), though not shown, reveals that the levels of largely Ge 4s-orbital character occur about 4 eV below the Fermi level, and those of largely Ge 4p-orbital character start to occur well above the Fermi level. Consequently, the oxidation state of Ge is best described by +2. Since the Ge contribution to the partially filled band is negligible, the use of the rigid band scheme (i.e., the use of $Nb_3GeTe_6^{0.4+}$ for $Nb_3Ge_{0.9}Te_6$) is justified.

(10) Whangbo, M.-H.; Hoffmann, R. *J. Am. Chem. Soc.* **1978**, *100*, 6093.
(11) The Ge parameters used were: $H_{ii} = -16$ eV and $\zeta = 2.16$ for the 4s orbital, and $H_{ii} = -6.86$ eV and $\zeta = 1.85$ for the 4p orbital.

Table I. Te···Te Contact Distances and Their Overlap Populations of Nb_3GeTe_6 Calculated with the Fermi Level Appropriate for $Nb_3Ge_{0.9}Te_6$

class	contact	distance[a] (Å)	overlap pop. (e^-/bond)
intralayer	Te(1)–Te(2)	3.338 (×8)	0.018
	Te(3)–Te(3)	3.582 (×8)	0.002
	Te(2)–Te(3)	3.616 (×8)	0.001
	Te(2)–Te(2)	3.647 (×8)	−0.030
	Te(1)–Te(1)	3.744 (×4)	−0.028
	Te(2)–Te(3)	3.764 (×4)	−0.002
	Te(3)–Te(3)	3.782 (×4)	−0.018
	Te(2)–Te(3)	3.836 (×8)	−0.003
	Te(1)–Te(1)	3.846 (×8)	−0.005
interlayer	Te(2)–Te(2)	3.766 (×4)	0.013
	Te(1)–Te(3)	3.803 (×8)	0.009
	Te(1)–Te(2)	3.830 (×8)	0.006

[a] The numbers in parentheses refer to the number of contacts per unit cell.

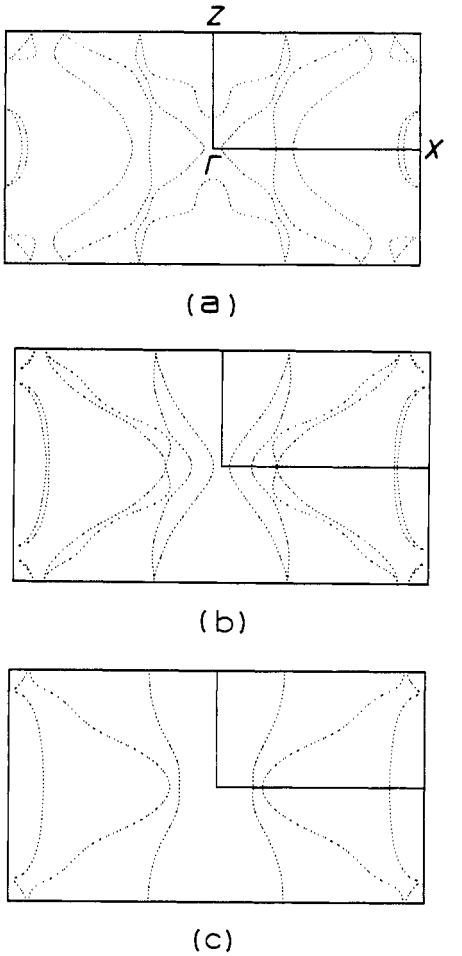

Figure 4. Cross sections of the Fermi surfaces of Nb_3GeTe_6, cut at the b^*-height of (a) 0.0, (b) $0.3b^*$, and (c) $0.5b^*$, parallel to the a^*c^*-plane. In part a, $\Gamma = (0, 0, 0)$, $X = (a^*/2, 0, 0)$, and $Z = (0, 0, c^*/2)$. The Fermi level employed is the one appropriate for $Nb_3Ge_{0.9}Te_6$.

Our extended Hückel molecular orbital calculations for the $Nb(1)Te_6$ single prism and the $Nb(2)Nb(3)Te_8$ double prism units of $Nb_3Ge_{0.9}Te_6$ show that one d-block level of the $Nb(1)Te_6$ single prism and two d-block levels of the $Nb(2)Nb(3)Te_8$ double prism units are lying low enough to be filled. In addition, our EHTB calculations for $Nb_3GeTe_6^{0.4+}$ show that the atomic populations of the Nb(1), Nb(2), and Nb(3) atoms are essentially identical. Thus, the oxidation states of all three Nb atoms are best described by 3+. With the oxidation state Ge^{2+}, the electron counting of Nb_3GeTe_6 is then given by $(Nb^{3+})_3(Ge^{+2})(Te^{1.833-})_6$, i.e., the state in which one electron is lost from six Te^{2-} ions. This suggests that the partially filled bands of Nb_3GeTe_6 should possess a substantial Te p-orbital character.

We now examine the orbital character of the partially filled bands. The partial DOS (PDOS) values of Nb, Ge, and Te calculated for Nb_3GeTe_6, shown in Figure 3a, reveals that the partially filled bands above the Fermi level are represented almost equally by the Nb d and the Te p orbitals. The contribution of the Te p_z orbitals (perpendicular to the plane of the layer) to the PDOS of Te is plotted in Figure 3b, according to which the Te contributions to the partially filled bands above the Fermi level are dominated by the Te p_z orbitals. Namely, the top part of the Te p_z-block bands is raised above the Fermi level in $Nb_3Ge_{0.9}Te_6$. Table I lists the overlap populations calculated for the short intra- and interlayer Te···Te contacts of $Nb_3Ge_{0.9}Te_6$. The intralayer contacts longer than 3.6 Å have either an extremely small positive or a negative overlap population, while all the interlayer contacts (longer than 3.7 Å) have positive overlap populations. Consequently, the short interlayer Te···Te contacts are crucial for the $p \rightarrow d$ electron transfer in Nb_3GeTe_6, as in the case of the CdI_2-type ditellurides MTe_2 (M = Ti, Nb, Ir).

Figure 2 predicts that $Nb_3Ge_xTe_6$ is a metal for a wide range of x values in the vicinity of 0.9 due to the presence of the partially filled bands. To examine the dimensionality of the metallic character in more detail, we calculate the Fermi surfaces[12] associated with these partially filled bands. Since the resulting Fermi surfaces are too complicated to be shown in a three-dimensional perspective view, we only consider their cross sections parallel to the a^*c^*-plane. Figure 4 shows the cross sections cut at the heights of 0.0, 0.3, and $0.5b^*$. Except for the height of $0.5b^*$, each cross section consists of a number of narrow closed loops, thereby showing that the electrical conductivity of Nb_3GeTe_6 should be good in the ac-plane. Above the height of $0.2b^*$, the middle two loops are elongated perpendicular to the a^*-direction, which therefore should provide a better electrical conductivity along the a-direction than along the c-direction. In addition, all closed loops become narrower with increasing the b^*-height and eventually collapse into lines at the height of $0.5b^*$. This means that the Fermi surfaces are closed along the b^*-direction, and hence a metallic character is predicted along the b-axis direction (i.e., the interlayer direction) as well. The latter is not surprising because the partially filled bands are largely made up of the Te p_z orbitals, by which the adjacent layers of $Nb_3Ge_{0.9}Te_6$ interact along the b-axis direction. According to the Fermi surfaces of Figure 4, the electrical conductivity of $Nb_3Ge_{0.9}Te_6$ should be strongest along the a-axis direction and weakest along the b-axis direction. The Fermi surfaces calculated for $Nb_3Ge_xTe_6$ as a function of x (not shown) reveal that the conductivity anisotropy in the ac-plane gradually diminishes as x approaches the stoichiometric value of 1.0.

Acknowledgment. This work was in part supported by the U.S. Department of Energy, Office of Basic Sciences, Division of Materials Sciences, under Grant DE-FG05-86ER45259, by NATO, Scientific Affairs Division, and by Centre National de la Recherche Scientifique.

(12) For a recent review on Fermi surfaces, see: Canadell, E.; Whangbo, M.-H. *Chem. Rev.* **1991**, *91*, 965.